Modeling of laser wakefield acceleration at CO_2 laser wavelengths

N. E. Andreev, S.V. Kuznetsov, and A. A. Pogosova
Institute for High Energy Densities, Russian Academy of Sciences, Izhorskaya 13/19, Moscow 125412, Russia

L. C. Steinhauer
Redmond Plasma Physics Laboratory, University of Washington,
14700 NE 95th Street, Suite 100, Redmond, Washington 98052, USA

W. D. Kimura*
STI Optronics, Inc., 2755 Northup Way, Bellevue, Washington 98004, USA
(Received 4 February 2003; published 29 April 2003)

The upgraded Accelerator Test Facility (ATF) CO_2 laser located at Brookhaven National Laboratory offers a unique opportunity to investigate laser wakefield acceleration (LWFA) with a 10.6-μm laser, a wavelength where little experimental work exists. While long laser wavelengths have certain advantages over short wavelengths, our modeling analysis has uncovered another important effect. The upgraded ATF CO_2 laser will have a pulse length as short as 2 ps. At a nominal plasma density of $\sim 10^{16}$ cm^{-3}, this pulse length would normally be considered too long for resonant LWFA, but too short for self-modulated LWFA. However, our model simulations indicate that a well-formed wakefield is nevertheless generated with electric field gradients of $E_z \gtrsim 2$ GV/m assuming 2.5 TW laser peak power. The model indicates pulse steepening is occurring due to various nonlinear effects. It is possible that this intermediate laser pulse length mode of operation may permit the creation of well-formed, regular-shaped wakefields, which would be needed for staging the LWFA process. Discussed in this paper are the model, its predictions for an LWFA experiment at the ATF, and the pulse steepening effect.

DOI: 10.1103/PhysRevSTAB.6.041301 PACS numbers: 41.75.Jv, 52.38.Kd, 42.55.Lt

I. INTRODUCTION

Laser wakefield acceleration (LWFA), whereby a high-intensity laser pulse creates a plasma wake that can accelerate electrons, has demonstrated very high acceleration gradients of over 1 GV/m [1]. Most of the experiments to date, however, have used near-infrared laser sources (e.g., $\lambda \approx 1$ μm) where terawatt (TW) peak powers are readily available. It has been noted [2–4] that longer laser wavelengths have certain advantages. These advantages have not been explored experimentally because of the lack of a long-wavelength TW laser source with the proper pulse length needed to drive the wake.

The Accelerator Test Facility (ATF) located at Brookhaven National Laboratory (BNL) is upgrading their CO_2 laser to deliver multi-TW output power [5]. The previous laser [6] consisted of a CO_2 laser oscillator, a 5-atm regenerative CO_2 preamplifier, and a 9-atm CO_2 laser amplifier. This system produced > 5 J output energies with a pulse length of approximately 180 ps. For the upgrade, the preamplifier has been replaced with a 10-atm device. This higher pressure causes the CO_2 gain spectrum to be more uniform over frequency, thereby enabling amplification of very short laser pulses without the generation of daughter pulses. It is anticipated that the upgraded system will be able to produce 2–10 ps laser pulses with the same 5-J pulse energy corresponding to a maximum peak power of 2.5 TW.

The availability of this upgraded laser source opens up the possibility to perform LWFA experiments at 10.6 μm. In addition, the ATF has also been performing capillary discharge experiments where they have demonstrated channeling of the CO_2 laser light [7]. Capillary discharges have demonstrated plasma lengths of many centimeters [8]. Thus, the ATF not only possesses a viable laser driver for LWFA, but also a means to perform acceleration over many Rayleigh lengths.

The purpose of the modeling analysis and results presented in this paper is to predict the performance of a LWFA experiment performed at the ATF using the upgraded laser. This will provide a guide in planning such an experiment. This experiment would be one of the first to examine LWFA at 10.6 μm over plasma lengths of many centimeters. As we will show, for the conditions of the upgraded ATF CO_2 laser, electric field gradients of $E_z \gtrsim 2$ GV/m are possible.

During the process of our modeling analysis we also uncovered another noteworthy feature of this experiment. At a plasma density of $n_e \sim 10^{16}$ cm^{-3}, the 2-ps laser pulse is considered too long for the optimum generation of a plasma wake via so-called resonant LWFA [9,10]. Resonant LWFA normally requires the laser pulse length τ_p to be comparable or less than half of the plasma wake period π/ω_p, where $\omega_p \propto n_e^{1/2}$ is the plasma frequency.

*Corresponding author: wkimura@stioptronics.com

At $n_e = 10^{16}$ cm^{-3}, this corresponds to ≈ 0.4 ps. On the other hand, self-modulated LWFA [11–20] normally requires laser pulse lengths substantially longer than 2 ps. Longer pulses allow the wake to grow via Raman forward scattering or a resonant modulation instability within the laser pulse envelope. A 2-ps pulse means the laser pulse terminates before these processes have had time to fully develop.

What we found is that the 2-ps laser pulse still generates a well-formed, regular wake with a surprisingly strong electric field gradient of $\gtrsim 2$ GV/m. Formation of regular wakes is one prerequisite for staging LWFA devices in series. Staging would be important for eventually developing practical accelerators based upon LWFA.

In this paper we describe the LWFA model, its modifications for simulating the ATF CO_2 laser, and its predictions for an LWFA experiment that could be performed at the ATF. We conclude with a discussion of the results.

II. DESCRIPTION OF BASIC LWFA MODEL WITH MODIFICATIONS RELATED TO CO_2 LASERS

To describe the laser pulse propagation in a plasma channel we use the following Maxwell's wave equation for the complex pulse amplitude a (see, e.g., [21,22]):

$$\left\{2ik_0\left(\frac{\partial}{\partial z} + c^{-1}\frac{\partial}{\partial t}\right) + \Delta_\perp + \frac{\partial^2}{\partial z^2} - c^{-2}\frac{\partial^2}{\partial t^2}\right\}a = k_0^2 \frac{n}{n_c \gamma} a, \tag{1}$$

where n is the density of the plasma electrons, $n_c = m\omega_0^2/4\pi e^2$ is the critical electron density (m and e are the electron mass and charge, respectively), ω_0 is the laser frequency, and $\Delta_\perp$ is the transverse part of the Laplace operator. The dimensionless envelope amplitude of the laser pulse a [slowly varying on the time and spatial scales ω_0^{-1} and $k_0^{-1} = c/\omega_0$ (c is the speed of light), which are the inverse frequency and wave number of the laser radiation, respectively] is related to the electric field of the laser pulse $\mathbf{E}_0$ by the expression

$$e\mathbf{E}_0/(m\omega_0 c) = \mathrm{Re}\{\mathbf{e}_0 a \exp[-i\omega_0 t + ik_0 z]\}. \tag{2}$$

Here $\mathbf{e}_0$ is the unit vector of the laser polarization, which is assumed to be linear. We consider an axisymmetric geometry with an axisymmetric laser pulse propagating along the axis of a cylindrical plasma channel. The slowly varying electron plasma density n describes the nonlinear plasma response to the ponderomotive action of the laser pulse, namely, the wakefield generation, and γ is the averaged relativistic factor of the electrons [21], i.e.,

$$\gamma = \left[1 + \left(\frac{\mathbf{p}}{mc}\right)^2 + \frac{1}{2}|a|^2\right]^{1/2}, \tag{3}$$

where $\mathbf{p}$ is the electron momentum connected with the velocity of the electrons by the relation $\mathbf{v} = \mathbf{p}/(m\gamma)$. In deriving Eq. (1), the scale of the plasma inhomogeneity is assumed to be larger than the wavelength of the laser radiation.

To describe the slowly varying (on the time scale ω_0^{-1}) motions and fields in the plasma we use Maxwell's equations and the relativistic hydrodynamic equations for cold plasma electrons:

$$\frac{\partial \mathbf{p}}{\partial t} = e\mathbf{E} - mc^2\nabla\gamma, \tag{4}$$

$$\frac{\partial n}{\partial t} + div(n\mathbf{v}) = 0, \tag{5}$$

$$\frac{\partial \mathbf{E}}{\partial t} = -4\pi en\mathbf{v} + c \cdot rot\mathbf{B}, \tag{6}$$

$$rot\mathbf{E} = -\frac{1}{c}\frac{\partial \mathbf{B}}{\partial t}. \tag{7}$$

Here Eq. (4) follows from Eq. (3) of Ref. [21] and the recognition that the generalized electron vorticity $\nabla \times (\mathbf{p} - e\mathbf{A}/c)$, which is zero initially, should always remain zero [23].

For laser pulses not too long (but still of interest) plasma ions can be treated as an immobile neutralizing background. A characteristic time for the ion density modification in ambipolar plasma motion under the action of a ponderomotive force in the radial direction can be estimated from the equation for the ion density N:

$$\frac{1}{N_0(r)}\frac{\partial^2 N}{\partial t^2} = \mu c^2 \Delta_\perp \gamma, \tag{8}$$

where $N_0(r) = N(t = 0, r)$ is the initial unperturbed density of ions, $\mu = mZ/M$, and Z and M are the charge number and mass of the ions, respectively. From this equation for a laser pulse with a Gaussian profile in the radial direction with transverse scale r_L, the characteristic time for a pronounced ion density modification is

$$t_{\mathrm{ion}} \approx \frac{1}{\sqrt{\mu}}\frac{r_L}{c} a_0^{-1}, \tag{9}$$

where a_0 is the maximum of the laser field envelope. For the range of parameters under consideration, $r_L \approx 100\ \mu$m, $a_0 \approx 1$, and $\mu \approx 5 \times 10^{-4}$; the estimate from Eq. (9) then gives $t_{\mathrm{ion}} \approx 15$ ps. This is much longer than the 2-ps CO_2 laser pulse duration of interest and permits us to neglect (in the first approximation) the ion motion.

The equations can be simplified into a form for a single scalar potential function as follows. In the quasistatic approximation [24] by using dimensionless coordinates moving with the laser pulse variables

$$\xi = k_{p0}(z - ct), \qquad \zeta = k_{p0}z, \qquad \boldsymbol{\rho} = k_{p0}\mathbf{r}_\perp, \tag{10}$$

the set of Eqs. (4)–(7) can be written in the form:

$$\frac{\partial}{\partial \xi}(\mathbf{e}_z \gamma - \mathbf{q}) = \mathbf{E} - \nabla_\perp \gamma, \tag{11}$$

$$\frac{\partial}{\partial \xi}[(u_z - 1)\nu] + \partial_\perp(\nu \boldsymbol{u}_\perp) = 0, \tag{12}$$

$$\left[\frac{\partial^2 \mathbf{E}}{\partial \xi^2} + \nabla \times \nabla \times \mathbf{E}\right] = \frac{\partial}{\partial \xi}(\nu \mathbf{u}), \tag{13}$$

where $\nu = n/N_0$ is the normalized electron density, [the constant N_0 will be chosen later as the unperturbed electron plasma density on the channel axis $N_0 = n_0(r = 0)$]; $k_{p0} = \omega_{p0}/c = (4\pi e^2 N_0/m)^{1/2}/c$ is a normalizing inverse space scale; $\nabla_\perp$ and $\partial_\perp$ are the transverse parts of the gradient and divergence, respectively; and $\mathbf{q} = \mathbf{p}/mc$, $\mathbf{u} = \mathbf{v}/c$, and $\mathbf{E} \Rightarrow e\mathbf{E}/(mc\omega_{p0})$ are consequently the dimensionless electron momentum, velocity, and slowly varying electric field, respectively. The nonlinear relativistic plasma response ν/γ can be expressed in accordance with Eqs. (11)–(13) through a single scalar function (potential) Φ (compare [25]):

$$\frac{\nu}{\gamma} = \frac{\nu_0 + \Delta_\perp \Phi}{\Phi}, \tag{14}$$

where $\nu_0 = n_0(r)/N_0$ is the normalized electron background density in the plasma channel and the potential $\Phi = \gamma - q_z$ is defined with the boundary condition $\Phi(\xi \to +\infty) = 1$.

The dimensionless components of the electric and magnetic fields in the plasma, and thus the forces acting on an accelerated relativistic electron, can be also expressed through the dimensionless potential $\Phi \Rightarrow m_e c^2 \Phi/e$:

$$F_z = E_z = \frac{\partial \Phi}{\partial \xi}, \qquad F_r = E_r - B_\varphi = \frac{\partial \Phi}{\partial \rho}, \tag{15}$$

where in the last expression axisymmetry is assumed. The equation for the potential can be obtained from Eqs. (11)–(13) taking into account Eqs. (14) and (15). The simplification of this equation is possible for a broad laser pulse (compared with the plasma skin depth $1/k_{p0}$), or for intensities of the laser pulse smaller than relativistic ones ($|a| \ll 1$). In these cases the equation for the potential can be linearized with respect to the small parameter $|\Phi - 1|/(k_{p0} r_L)^2$, where r_L is the transverse scale of the laser pulse envelope. In doing so we arrive at the following equation for the potential:

$$\begin{aligned}&\bigg\{(\Delta_\perp - \nu_0)\frac{\partial^2}{\partial \xi^2} - \frac{\partial \ln \nu_0}{\partial \rho}\frac{\partial^3}{\partial \rho \partial \xi^2} \\ &\quad + \nu_0 \Delta_\perp\bigg\}\Phi - \frac{\nu_0^2}{2}\left[1 - \frac{1 + |a|^2/2}{\Phi^2}\right] = \frac{\nu_0}{4}\Delta_\perp |a|^2. \end{aligned} \tag{16}$$

This equation has two exact limits. (i) The fully relativistic 1D limit is when $|\Phi - 1|/(k_p r_L)^2 \ll 1$ and all transverse derivatives can be neglected. In this limit Eq. (16) reduces to $(\partial^2\Phi/\partial\xi^2) + (\nu_0/2)[1 - ([1 + |a|^2/2]/\Phi^2)] = 0$. (ii) The linear limit when $|a|^2 \ll 1$, $|\Phi - 1| \ll 1$, and Eq. (16) can be transformed into Eq. (8) of Ref. [26].

In the same dimensionless coordinates moving with the laser pulse variables [i.e., Eq. (10)], Eq. (1) has the form

$$\left\{2i\frac{\partial}{\partial \zeta} + \frac{k_{p0}}{k_0}\left(\Delta_{\perp\rho} + 2\frac{\partial^2}{\partial \zeta \partial \xi}\right)\right\}a = \frac{k_{p0}}{k_0}\frac{\nu}{\gamma}a, \tag{17}$$

where a small second derivative on variable ζ is omitted. Further we shall assume that the restriction $|\Phi - 1|/(k_p r_L)^2 < 1$ is fulfilled and shall use Eqs. (14), (16), and (17) to analyze the intense CO_2 laser pulse channeling and wakefield generation in wide plasma channels.

III. MODEL PREDICTIONS

In accordance with the anticipated parameters of the upgraded ATF CO_2 laser, the laser parameters assumed in the numerical modeling are listed in Table I. The laser pulse is focused at the entrance of the plasma channel where it is assumed to be Gaussian in both space (radial direction) and time,

$$a(r, z = 0, t) = a_0 \exp\left[-\frac{r^2}{2r_L^2} - \frac{\pi}{2}\frac{t^2}{\tau_L^2}\right]. \tag{18}$$

TABLE I. BNL ATF laser parameters used in the model simulation.

Parameters	Value
Laser wavelength, λ (μm)	10.6
Laser pulse duration, τ_L (ps)	2
Laser peak power, P_L (TW)	2.5
Laser pulse energy, E_L (J)	5
Laser pulse radius at vacuum focus, r_L (μm)	101
Laser beam Rayleigh length, Z_R (mm)	6.07
Normalized laser field strength at vacuum focus, a_0	0.8
Plasma channel radius (μm)	202
Plasma channel length (cm)	6.7

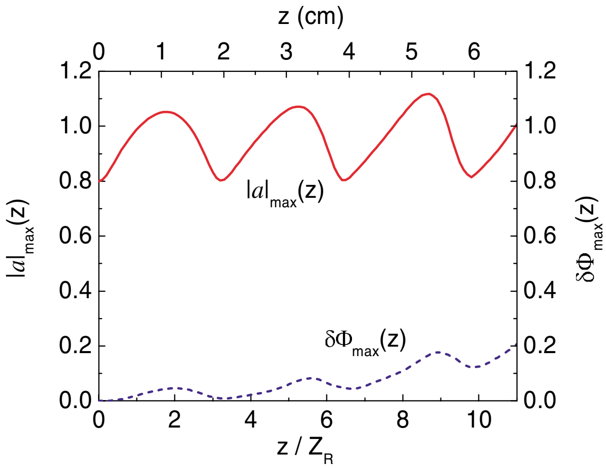

FIG. 1. (Color) The maxima of the laser pulse field on axis $|a(r=0,z)|_{\max}$ (solid line) and the maximum of the wakefield potential $\delta\Phi_{\max}(r=0,z)=\Phi_{\max}(r=0,z)-1$ behind the pulse (dashed line) versus propagation distance z (normalized to the Rayleigh length $Z_R=k_0r_L^2$ and in cm). The laser spot radius $r_L=101\ \mu$m, laser field $a_0=0.8$, and channel radius $R_{\rm ch}=202\ \mu$m (see Table I for other parameter values).

The plasma channel is assumed to be parabolic,

$$n_0(r)=n_0(r=0)\left[1+\frac{r^2}{R_{\rm ch}^2}\right], \tag{19}$$

with the electron plasma density on the axis $N_0=n_0(r=0)=1.1\times10^{16}\ \mathrm{cm}^{-3}$ (corresponding to $\gamma_g\equiv\omega_0/\omega_{p0}=30$). The channel radius is matched with the initial laser spot size by the linear condition [27]

$$R_{\rm ch}=k_{p0}r_L^2, \tag{20}$$

which in the case of the electron density profile, Eq. (19), provides guided propagation of a Gaussian laser pulse without substantial distortion for a moderate laser power, $P_L/P_c\ll1$ (where P_c is the critical power for relativistic self-focusing in a plasma, $P_c\cong17(\omega_0/\omega_{p0})^2$[GW]). Note that for the foregoing parameters (i.e., $P_L=2.5$ TW, $N_0=1.1\times10^{16}\ \mathrm{cm}^{-3}$), $P_L/P_c=0.16$.

Figures 1–5 illustrate the laser pulse propagation and wakefield generation for a laser pulse spot size at the entrance of the plasma channel of $r_L=101\ \mu$m, a normalized maximum of the laser field $a_0=0.8$ (corresponding to a laser intensity $q_L=0.78\times10^{16}\ \mathrm{W/cm^2}$), and a channel radius $R_{\rm ch}=202\ \mu$m.

IV. DISCUSSION OF RESULTS

In Fig. 1, the small fluctuation in the laser field corresponds to a modulation in the laser envelope. This modulation is the result of a slight difference from the perfectly matched channel size, Eq. (20), as discussed in Ref. [27]. The period of the modulation is about π times the Rayleigh length $Z_R=k_0r_L^2$. The wakefield potential shown, $\delta\Phi=\Phi-1$, represents its value behind the laser pulse as a function of the propagation distance z (normalized to the Rayleigh length). This wakefield potential shows considerable growth by the end of the distance shown in the figure ($z\sim7$ cm). Since the normalization for the potential is $mc^2/e=0.511$ MV, the magnitude of

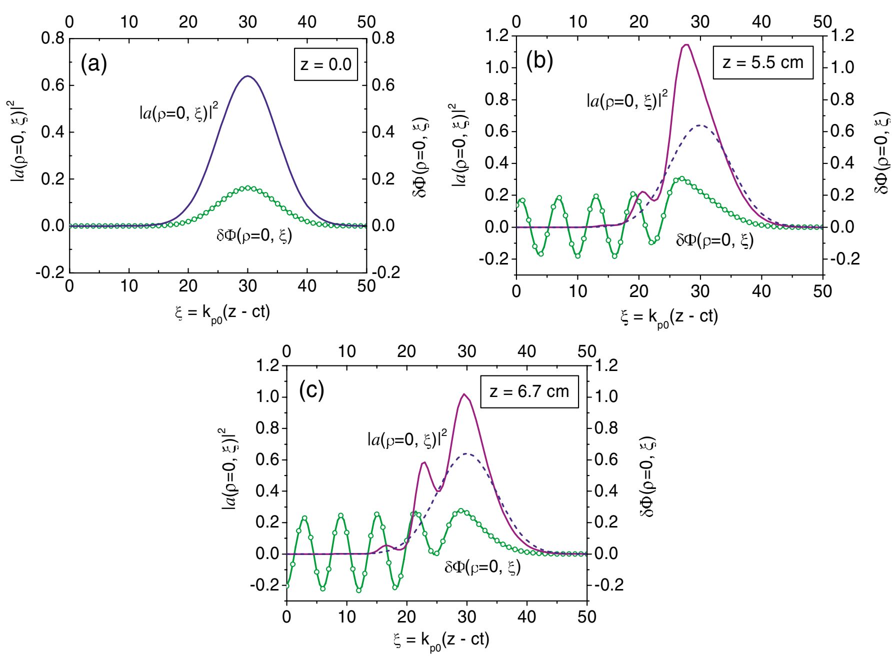

FIG. 2. (Color) The normalized laser pulse intensity on axis $|a(r=0,\xi)|^2$ and wakefield potential $\delta\Phi=\Phi(r=0,\xi)-1$ (lines marked by circles) at propagation distances (a) $z=0$, (b) $z=5.5$ cm, and (c) $z=6.7$ cm. The parameters are the same as in Fig. 1.

the wake potential at this point is about 0.1 MV. Hence, the resulting wakefield $E_z \sim k_{p0}\delta\Phi$ is about 2 GV/m.

Even though the 2-ps laser pulse duration is much longer than that for "resonant" LWFA (0.4 ps for the density in this example), a very strong wake is generated. This is a result of the nonlinear evolution of the laser pulse because of the coupling with the plasma. The coupled evolution of the laser and wakefields is shown in Fig. 2 for various positions in the plasma. At the entrance to the plasma (Fig. 2, $z = 0$), the laser field is in its initial, unperturbed state, and the wakefield simply reflects the presence of the laser field. At a distance of $z =$ 5.5 cm into the plasma [Fig. 2(b)], a significant wake is trailing behind (to the left of) the laser pulse. A key feature is that the laser pulse itself has been modified; the solid line is the laser field at this point and the dashed line is what the field would be if it were unchanged. The peak laser field has increased. The higher peak field reflects the modulation of the envelope (see Fig. 1), and at this point $|a|^2_{\max}$ is more than 50% higher than its initial value.

A more important effect, however, in terms of wake generation is the nonlinear pulse steepening, which arises from two effects. First, stronger self-focusing at the middle (maximum) of the laser pulse produces pulse steepening [27]. Second, a growing modulation has appeared near the trailing edge of the pulse. As a result of the modulation, the local gradient of the field $d|a|^2/d\xi$ has become quite steep. This causes the pulse to act as if it has a much shorter length, i.e., behave much closer to the resonant condition for LWFA. These effects, as well as the processes of self-phase modulation and group velocity dispersion, also cause a shift in the laser pulse maximum toward the back of the pulse and a precipitous drop after the peak [22]. These "pulse shortening" effects enable the relatively long overall pulse to generate a strong wake. Observe that only a short distance farther into the plasma at $z = 6.7$ cm [Fig. 2(c)], the laser field modulation near the pulse trailing edge has rapidly become stronger and crept deeper into the pulse. We should note that nonlinear pulse steepening has been observed in experiments with a Ti:sapphire laser [28] in which a strong wake was generated even though the initial laser pulse length was a factor of ~2.5 too long for efficient wake excitation.

The radial and longitudinal structure of the laser field, electron density, and wake potential are shown in Figs. 3–5, respectively, at a distance $z = 6.7$ cm. The density modulation (Fig. 4) has very large amplitudes with peak densities on axis more than 100% above the ambient density. Note in Fig. 4 that the laser pulse center is at about $\xi \sim 30$ and toward the left on the figure, so that the large density fluctuations are mainly behind the pulse. The wake potential (Fig. 5) has a large first peak, mainly because of the presence of the laser pulse, but a strong fluctuating wake is left behind the pulse. Here the laser pulse center $\xi \sim 30$ is towards the right in Fig. 5.

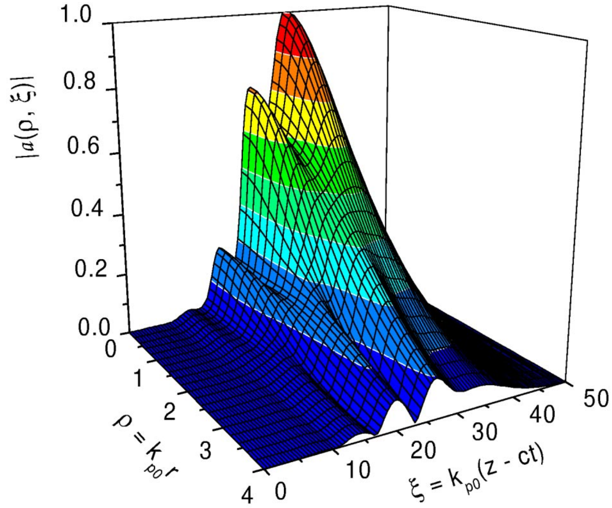

FIG. 3. (Color) The normalized laser field $|a(\rho, \xi)|$ after 6.7 cm propagation. The parameters are the same as in Fig. 1.

Model simulations have also been performed for the situation of a broader profile, i.e., a broader laser spot size and wider channel. The laser spot at the entrance of the plasma channel is $r_L = 115$ μm, and the channel radius is $R_{ch} = 259$ μm. For this example the normalized maximum of the laser field is lower, $a_0 = 0.707$, corresponding to a laser intensity $q_L = 0.61 \times 10^{16}$ W/cm^2. This simulation was carried out for a longer propagation distance into the plasma of 13.2 cm, than the $z = 6.7$ cm in the example of Figs. 1–5.

The results appear very similar to those shown in Figs. 1–5, but with a few noteworthy differences. In the broader laser spot example the modulation of $|a|_{\max}(z)$ is slower because of the wider channel and longer Rayleigh length. Although the peak laser field $|a|_{\max}$ is about 20% lower in this case (see Fig. 2), the laser pulse modulation

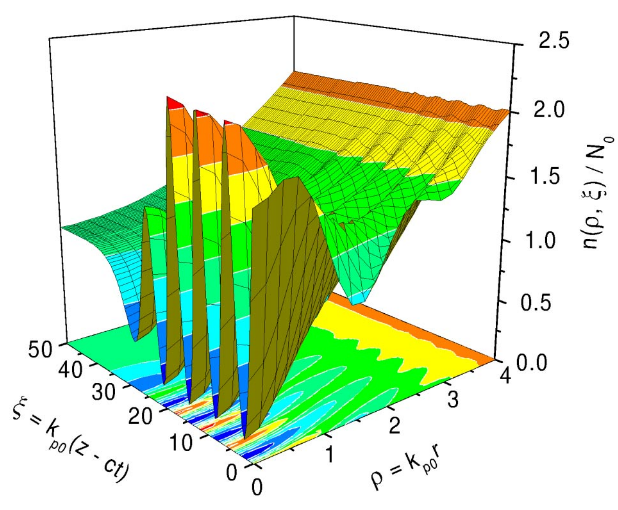

FIG. 4. (Color) Electron plasma density $n(\rho, \xi)/N_0$ after 6.7 cm propagation. The parameters are the same as in Fig. 1.

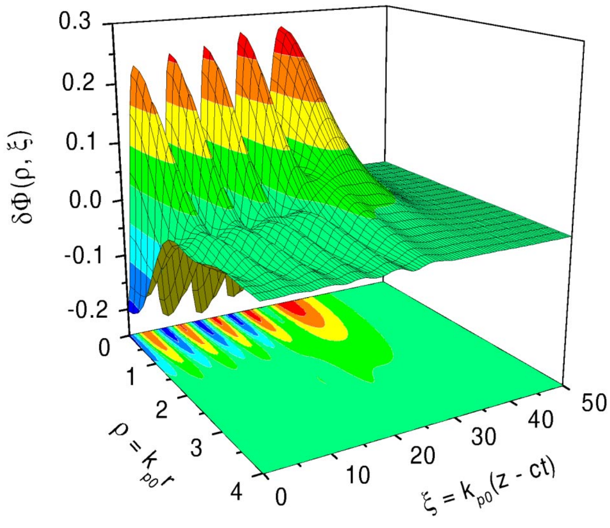

FIG. 5. (Color) The wakefield potential $\delta\Phi = \Phi(\rho, \xi) - 1$ after 6.7 cm propagation. The parameters are the same as in Fig. 1.

is deeper and the wake potential is larger because of the greater propagation distance into the plasma. Under this situation the normalized wake potential Φ is $\sim$0.28, corresponding to an electric field of $E_z \sim 2.8$ GV/m.

This comparison of different laser spot sizes shows that a broader laser spot (and corresponding channel radius) leads to a broader wakefield. The wakefield grows more slowly, but continues to grow with propagation distance into the plasma. An increase of the transverse scale of the wakefield may be preferable for the acceleration of finite-sized electron bunches due to a decrease of the radial forces and prevention of transverse wave breaking of the plasma wake.

V. CONCLUSION

The principal result of this analysis is that a strong wake is excited even though the original laser pulse length is several times too long for efficient wake excitation by resonant LWFA. This arises because of nonlinear laser-electron coupling effects, which lead to an effective pulse steepening. The pulse steepening arises from the stronger self-focusing at the middle (peak) of the laser pulse and a growing self-modulation of the pulse after its peak. The resultant steepening causes the pulse to act as if it has a shorter duration.

A consequence of this pulse steepening effect is that the terawatt upgrade of the CO_2 laser at the ATF will enable unique LWFA experiments to be performed. These would be one of the first to demonstrate LWFA at 10.6 μm. Furthermore, they may also demonstrate acceleration over an extended interaction length of $\sim$10 cm using a capillary discharge plasma for laser channeling. Simulations predict a wake amplitude > 1 GV/m for a 2-ps, 2.5-TW laser pulse. A properly phased particle accelerated in this wake over 10 cm would gain > 100 MeV energy.

ACKNOWLEDGMENTS

This work was supported by the U.S. Department of Energy, Grant No. DE-FG03-98ER41061, and partially by the Russian Foundation for Basic Research, Grant No. 01-02-16723.

[1] See, for example, W. P. Leemans and E. Esarey, in *Proceedings of Advanced Accelerator Concepts 8th Workshop, Baltimore, MD, 1998*, edited by W. Lawson, C. Bellamy, and D. Brosius, AIP Conf. Proc. No. 472 (AIP, New York, 1999), p. 174; D. Gordon, K. C. Tzeng, C. E. Clayton, A. E. Dangor, V. Malka, K. A. Marsh, A. Modena, W. B. Mori, P. Muggli, Z. Najmudin, D. Neely, C. Danson, and C. Joshi, Phys. Rev. Lett. **80**, 2133 (1998); C. I. Moore, A. Ting, K. Krushelnick, E. Esarey, R. F. Hubbard, B. Hafizi, H. R. Burris, C. Manka, and P. Sprangle, Phys. Rev. Lett. **79**, 3909 (1997).

[2] I. V. Pogorelsky, Nucl. Instrum. Methods Phys. Res., Sect. A **410**, 524 (1998).

[3] N. E. Andreev, S. V. Kuznetsov, and I. V. Pogorelsky, Phys. Rev. ST Accel. Beams **3**, 021301 (2000).

[4] L. C. Steinhauer, W. D. Kimura, N. E. Andreev, S. V. Kuznetsov, and A. A. Pogosova, in *Advanced Accelerator Concepts, Mandalay Beach, CA, 2002*, edited by C. E. Clayton and P. Muggli, AIP Conf. Proc. No. 647 (AIP, New York, 2002), pp. 751–759.

[5] I. V. Pogorelsky, I. Meshkovsky, A. Dublov, I. Pavlishin, Yu. A. Boloshin, G. B. Deineko, and A. Tsunemi, in *Proceedings of LASERS's 98, Tucson, AZ, 1998*, edited by V. J. Corcoran and T. A. Goldman (STS Press, McLean, VA, 1999), p. 911.

[6] I. V. Pogorelsky, J. Fischer, K. P. Kusche, M. Babzien, N. A. Kurnit, I. J. Bigio, R. F. Harrison, and T. Shimada, IEEE J. Quantum Electron. **31**, 556 (1995).

[7] I. V. Pogorelsky, I. Ben-Zvi, T. Hirose, V. Yakimenko, K. Kusche, P. Siddons, T. Kumita, Y. Kamiya, F. Zhou, A. Zigler, B. Greenberg, D. Kaganovich, I. V. Pavlichine, A. Diublov, N. Andreev, N. Bobrova, and P. Sasorov, "Primary Tests of Laser/*e*-Beam Interaction in a Plasma Channel," 10th Workshop on Advanced Accelerator Concepts, 2002, Mandalay Beach, CA (unpublished).

[8] A. Zigler, B. Greenberg, T. Palhan, D. Kaganovich, R. F. Hubbard, A. Ting, T. G. Jones, and P. Sprangle, in *Advanced Accelerator Concepts, Mandalay Beach, CA, 2002* (Ref. [4]), pp. 47–53.

[9] T. Tajima and J. M. Dawson, Phys. Rev. Lett. **43**, 267 (1979).

[10] L. M. Gorbunov and V. I. Kirsanov, Sov. Phys. JETP **66**, 290 (1987).

[11] N. E. Andreev, L. M. Gorbunov, V. I. Kirsanov, A. A. Pogosova, and R. R. Ramazashvili, Pis'ma Zh. Eksp. Teor. Fiz. **55**, 551 (1992) [JETP Lett. **55**, 571–576 (1992)].

[12] T. M. Antonsen, Jr. and P. Mora, Phys. Rev. Lett. **69**, 2204 (1992).

[13] P. Sprangle, E. Esarey, J. Krall, and G. Joyce, Phys. Rev. Lett. **69**, 2200 (1992).

[14] J. Krall, A. Ting, E. Esarey, and P. Sprangle, Phys. Rev. E **48**, 2157 (1993).

[15] W. B. Mori, C. D. Decker, D. E. Hinkel, and T. Katsouleas, Phys. Rev. Lett. **72**, 1482 (1994).

[16] E. Esarey, J. Krall, and P. Sprangle, Phys. Rev. Lett. **72**, 2887 (1994).

[17] E. Esarey, P. Sprangle, J. Krall, and A. Ting, IEEE Trans. Plasma Sci. **24**, 252 (1996).

[18] N. E. Andreev, L. M. Gorbunov, V. I. Kirsanov, and A. S. Sakharov, IEEE Trans. Plasma Sci. **24**, 363 (1996).

[19] C. D. Decker, W. B. Mori, K-C. Tzeng, and T. C. Katsouleas, IEEE Trans. Plasma Sci. **24**, 379 (1996).

[20] N. E. Andreev, L. M. Gorbunov, V. I. Kirsanov, A. A. Pogosova, and A. S. Sakharov, Plasma Phys. Rep. **22**, 379 (1996).

[21] P. Mora and T. M. Antonsen, Jr., Phys. Plasmas **4**, 217 (1997).

[22] N. E. Andreev, Y. Nishida, and N. Yugami, Phys. Rev. E **65**, 056407 (2002).

[23] L. C. Steinhauer and A. Ishida, Phys. Plasmas **5**, 2609 (1998).

[24] P. Sprangle, E. Esarey, and A. Ting, Phys. Rev. Lett. **64**, 2011 (1990).

[25] N. E. Andreev, E. V. Chizhonkov, A. A. Frolov, and L. M. Gorbunov, Nucl. Instrum. Methods Phys. Res., Sect. A **410**, 469 (1998).

[26] N. E. Andreev, L. M. Gorbunov, V. I. Kirsanov, K. Nakajima, and A. Ogata, Phys. Plasmas **4**, 1145 (1997)

[27] N. E. Andreev, L. M. Gorbunov, and V. I. Kirsanov, Phys. Plasmas **2**, 2573 (1995).

[28] S. Fritzler, V. Malka, E. Lefebvre, M.-M. Aleonard, F. Burgy, J.-P. Chambaret, J.-F. Chemin, K. Krushelnick, G. Malka, S. P. D. Mangles, Z. Najmudin, J.-P. Rousseau, J.-N. Scheurer, B. Walton, and A. E. Dangor, in *Advanced Accelerator Concepts, Mandalay Beach, CA, 2002* (Ref. [4]), pp. 54–62.